beginning of a new era in the equilibrium statistical-mechanical theory of melting/crystallization in polymers. We sense that the time is similar to the time of transition from the classical theories of critical points that began with Onsager's calculation[49] in the 1940s but which was not complete until the 1960s. As always in the statistical mechanics of cooperative phenomena, there is a need for more reliable and rigorous calculations for simple models. Without this fundamental work, there is little basis upon which to build theory. In addition, and this is what we have concentrated on in this paper, it appears that there is a need to rethink the question of what are the minimal features required in statistical-mechanical models of polymers. Studies along these lines are essential in directing calculational efforts away from unrealistic models and toward the more fruitful ones.

An alternative hypothesis to the Flory hypothesis is offered as a basis for future studies of polymer melting. The new hypothesis emphasizes the necessity for a volume expansion and an energy term in the model to account for the work done in the expansion. It is also necessary to consider more realistic lattice models which allow modeling of the detailed features of polymer chains because such details are essential in determining the thermodynamic properties of particular exactly solvable models. However, the introduction of more refined lattices without allowing a volume expansion does not appear promising. Even though our hypothesis suggests that extra features such as volume changes and attractive van der Waals interactions are required, it should be possible to accommodate such added features reasonably by using a long-range mean-field calculation. Thus, even with these apparent complications, there is hope that systematic study of the allowed conformational states of realistic three-dimensional lattice models will result in better theories of polymer melting.

Acknowledgment. This research was supported in part by a grant (DMR-8115979) to J.F.N. from the Condensed Matter Theory Section of the National Science Foundation.

Registry No. Polyethylene (homopolymer), 9002-88-4.

(49) Onsager, L. *Phys. Rev.* **1944**, *65*, 117.

ARTICLES

Ion–Molecule Reactions in Unsaturated Hydrocarbons: Allene, Propyne, Diacetylene, and Vinylacetylene

Vincent G. Anicich,* Geoffrey A. Blake, Jhong K. Kim,† Murray J. McEwan,‡ and Wesley T. Huntress, Jr.

Jet Propulsion Laboratory, California Institute of Technology, Pasadena, California 91109
(Received: August 16, 1983; In Final Form: May 23, 1984)

Ion–molecule reactions in allene, propyne, diacetylene, and vinylacetylene (1-buten-3-yne) have been studied at near-thermal energies by the technique of ion cyclotron resonance mass spectrometry. Rate coefficients and branching ratios are reported for the reactions of $C_3H_n^+$ (n = 1–4) with allene and propyne and for the reactions of $C_4H_n^+$ (n = 0–5) with diacetylene and vinylacetylene. Branching ratios are also given for the reactions of $C_4H_n^+$, C_5H_n, and $C_6H_n^+$ with propyne and for reactions of $C_6H_n^+$ with diacetylene and vinylacetylene. More than 90% of the reactive channels lead to product ions having a larger carbon skeleton than the reactant ion. Evidence for ions with the same m/e ratio having differing reactivities was obtained for $C_3H_3^+$, $C_6H_7^+$, and $C_7H_7^+$. Ion reaction sequences in allene and propyne were followed at higher pressures (10^{-4} torr) to investigate secondary, tertiary, and higher order processes.

Introduction

Previous studies of ion–molecule reactions in allene and propyne[1-4] have demonstrated that condensation reactions with subsequent loss of H atoms are common.

$$C_xH_y^+ + C_3H_4 \rightarrow C_{(x+3)}H_{(y+3)}^+ + H$$

Any single-step process that increases the size of the carbon skeleton in an ion or molecule may have relevance to the process of soot formation in hydrocarbon flames and to synthetic pathways for formation of complex molecules in intersteller clouds and in planetary atmospheres. Positive and negative ion have been observed in hydrocarbon flames,[5,6] and these will participate in condensation processes. Even in combustion flames of simple hydrocarbons such as acetylene, larger unsaturated hydrocarbon including allene, propyne, diacetylene, and vinylacetylene have been observed.[7,8] Although the relative importance of ion–molecule vs. radical mechanisms for production of the larger hydrocarbons is still uncertain, there is no doubt that ions do have an important role. When acetylene is subjected to a beam of 600-eV electrons, a range of polymerization products is observed.[9]

† Department of Chemistry, University of California, Irvine, CA 92717.
‡ NRC–NASA Senior Research Associate at JPL, 1980. On leave from the University of Canterbury, Christchurch, New Zealand.

(1) J. J. Myher and A. G. Harrison, *J. Phys. Chem.*, **72**, 1905 (1968).
(2) C. Lifshitz, Y. Gleitman, S. Gefen, U. Shainock, and I. Dotan, *Int. J. Mass Spectrom. Ion Phys.*, **40**, 1 (1981).
(3) C. Lifshitz and Y. Gleitman, *Int. J. Mass Spectrom. Ion Phys.*, **40**, 17 (1981).
(4) M. T. Bowers, D. D. Elleman, R. M. O'Malley, and K. R. Jennings, *J. Phys. Chem.*, **74**, 2583 (1970).
(5) R. Long, Report EPA-R3-72-020, 1972.
(6) A. N. Hayhurst and D. B. Kittelson, *Combust. Flame*, **31**, 37 (1978).
(7) K. H. Homann, J. Warnatz, and C. Wellmann, *Symp. (Int.) Combust., [Proc.]*, **16**, 853 (1977).
(8) Von H. J. Spangenberg, I. Borger, H. Hoffman, and G. Mogel, *Z. Phys. Chem. (Leipzig)*, **259**, 531 (1978).
(9) C. Willis, R. A. Back, and R. H. Morris, *Can. J. Chem.*, **55**, 3288 (1977).

0022-3654/84/2088-4608$01.50/0

TABLE I: $C_3H_n^+$ Reactions in Pure Allene[a]

	ΔH°_{298}, kJ mol^{-1}	$10^9 k_{exptl}$	$10^9 k_{ADO}$
$C_3H^+ + \text{allene} \longrightarrow C_4H_3^+ + C_2H_2$	(−495)	1.4	1.3
$C_3H_2^+ + \text{allene} \xrightarrow{0.04} C_4H_2^+ + C_2H_4$	−192		
$\xrightarrow{0.14} C_4H_3^+ + C_2H_3$	(−329)		
$\xrightarrow{0.50} C_4H_4^+ + C_2H_2$	−243	1.4	1.3
$\xrightarrow{0.09} C_5H_3^+ + CH_3$	−240		
$\xrightarrow{0.21} C_6H_5^+ + H$	−330		
$C_3H_3^{+\,b} + \text{allene} \longrightarrow$		⩽0.01	1.3
$C_3H_4^{+\,c} + \text{allene} \xrightarrow{0.05} C_4H_4^+ + C_2H_4$	−35		
$\xrightarrow{0.01} C_4H_6^+ + C_2H_2$	−104		
$\xrightarrow{0.01} C_5H_5^+ + CH_3$	−170	1.1	1.3
$\xrightarrow{0.07} C_6H_5^+ + H_2 + H$	53		
$\xrightarrow{0.87} C_6H_7^+ + H$	−256		

[a] Rate coefficients are expressed in units of cm^3 molecule^{-1} s^{-1}. [b] Unreactive form of $C_3H_3^+$ (see text). [c] Generated by ionization of allene. Assumed to have the allene structure.

The ion chemistry of acetylene has been studied extensively[10–19] and shows rapid condensation reactions with relatively large hydrocarbon species produced within a few reaction steps.

The present study is intended to extend the data base for ion–molecule condensation reactions to allene, propyne, diacetylene, and vinylacetylene.

Experimental Section

The experiments were performed using the ion cyclotron resonance (ICR) technique.[20] Although the ICR mass spectrometer at the Jet Propulsion Laboratory has been described previously,[16,21] several recent modifications will be reviewed. In the present work the vacuum chamber and magnet air gap have been reduced in size from 5.72 cm to 4.57 cm, resulting in an increase in the maximum magnetic field of the system from 1.2 T to 1.9 T. A "flat" ICR cell (1.27 cm × 2.54 cm cross section) is fitted between the magnet pole faces, and the pulse sequence and drift electrodes were configured for the McMahon–Beauchamp[21,22] trap-drift operation. All rate constants and branching ratios were measured in a 1.5-T magnetic field. A Bayard-Alpert ionization gauge was used to monitor the reactant gas pressure. The ionization gauge was calibrated with an M.K.S. Baratron capacitance manometer.

Measurements of reaction rate constants were made using the ion trap mode of operation. In this mode, the ion signal from the marginal oscillator was integrated over the drift pulse at known drift times for each repetition of the experiment. A base line without ions present was obtained by scanning the reaction time with the trapping plates at negative potentials. The ion-loss characteristics of the reaction cell were found by observing the reactant ion signal while scanning the reaction time in the absence of the reactant neutral species. The neutral reactant was then added to the cell, and the reactant ion signal was rescanned. From the ratio of these two signals (with and without the added neutral species) and the known gas pressure, the reaction rate constant was calculated.[22] The procedure has been automated using a Texas Instruments 990/10 minicomputer. The computer uses a digital-to-analog converter to step the experiment through the reaction time scan. Typically, the computer steps through the three scans at 10 predetermined reaction times and records the integrated ion signals using an analog-to-digital converter. An average at each step of typically 50 repetitions is made. The signal levels are then determined from the base-line measurement and the averaged ratio measurement. Smoothing of the ratio measurements is accomplished by a least-squares linear regression analysis of a semilog plot vs. time. The error limits of the resulting rate are determined from the statistics of averaging.

Product distributions were obtained by double-resonance ejection experiments in the drift mode of operation.[20] A Q-spoiler is used to measure the relative sensitivities of the marginal oscillator at the specific frequencies used.[23]

Allene and propyne gas were obtained from Linde Specialty Gas and were used without further purification. Diacetylene and vinylacetylene (1-buten-3-yne) were synthesized by standard methods.[24,25]

Results

Allene and Propyne. Reaction rates and branching ratios are reported for the reactions of $C_3H_n^+$ (n = 1–4) with allene in Table I and with propyne in Table II. Branching ratios for the reactions of $C_4H_n^+$, $C_5H_n^+$, $C_6H_n^+$, and $C_7H_n^+$ ($n \leq 7$) with propyne are reported in Tables III–VI. The data in Table I were obtained with pure allene, and the data in Tables II–V were obtained with pure propyne. The reactant ions in Table VI were derived from the parent gases listed, so that the reactions were examined in a mixture of propyne and the parent gas shown.

$C_3H_n^+$ ions (n = 1–4) react with both allene and propyne near the collision limit, with one exception. The $C_3H_3^+$ ion was observed to react only at short times. This behavior may imply that two

(10) M. S. B. Munson, *J. Phys. Chem.*, **69**, 572 (1965).
(11) G. A. W. Derwish, A. Galli, A. Giardini-Guidoni, and G. G. Volpi, *J. Am. Chem. Soc.*, **87**, 1159 (1965).
(12) J. H. Futrell and T. O. Tiernan, *J. Phys. Chem.*, **72**, 158 (1968).
(13) P. G. Miasek and J. L. Beauchamp, *Int. J. Mass Spectrom. Ion Phys.*, **15**, 49 (1974).
(14) R. H. Prince and G. R. Floyd, *Adv. Mass Spectrom.*, **6**, 773 (1974).
(15) M. Tsuji, T. Ogawa, T. Imasaka, Y. Nishimura, and N. Ishibashi, *Bull. Chem. Soc. Jpn.*, **49**, 53 (1976).
(16) J. K. Kim, V. G. Anicich, and W. T. Huntress, Jr., *J. Phys. Chem.*, **81**, 1798 (1977).
(17) F. W. Brill and J. R. Eyler, *J. Phys. Chem.*, **85**, 1091 (1981).
(18) Y. Ono and C. Y. Ng, *J. Chem. Phys.*, **77**, 2947 (1982).
(19) V. G. Anicich, W. T. Huntress, Jr., and M. J. McEwan, to be submitted for publication.
(20) T. A. Lehman and M. M. Bursey, "Ion Cyclotron Resonance Spectrometry", Wiley, New York, 1976.
(21) W. T. Huntress and R. F. Pinizzotto, *J. Chem. Phys.*, **59**, 4742 (1973).
(22) T. B. McMahon and J. L. Beauchamp, *Rev. Sci. Instrum.*, **43**, 509 (1972).
(23) V. G. Anicich and W. T. Huntress, Jr., *Rev. Sci. Instrum.*, **48**, 542 (1977).
(24) R. J. Tedeshi and A. E. Brown, *J. Org. Chem.*, **29**, 2051 (1964).
(25) P. D. Landor, S. R. Landor, and P. Leighton, *J. Chem. Soc., Perkin Trans. 1*, 1628 (1975).

TABLE II: $C_3H_n^+$ Reactions in Pure Propyne[a]

	ΔH°_{298}, kJ mol^{-1}	$10^9 k_{exptl}$	$10^9 k_{ADO}$
$C_3H^+ + \text{propyne} \longrightarrow C_4H_3^+ + C_2H_2$	(−488)	1.4	1.3
$C_3H_2^+ + \text{propyne} \xrightarrow{0.09} C_4H_2^+ + C_2H_4$	−185		
$\xrightarrow{0.12} C_4H_3^+ + C_2H_3$	(−322)		
$\xrightarrow{0.41} C_4H_4^+ + C_2H_2$	(−236)	1.3	1.3
$\xrightarrow{0.18} C_5H_3^+ + CH_3$	−233		
$\xrightarrow{0.20} C_6H_5^+ + H$	−323		
$C_3H_3^{+\,b} + \text{propyne} \longrightarrow$		⩽0.01	1.3
$C_3H_4^{+\,c} + \text{propyne} \xrightarrow{0.18} C_3H_5^+ + C_3H_3$	−86		
$\xrightarrow{0.02} C_4H_4^+ + C_2H_4$	−89		
$\xrightarrow{0.02} C_4H_6^+ + C_2H_2$	−158		
$\xrightarrow{0.02} C_5H_5^+ + CH_3$	−224	1.1	1.3
$\xrightarrow{0.08} C_6H_5^+ + H_2 + H$	−1		
$\xrightarrow{0.68} C_6H_7^+ + H$	−310		

[a] Rate coefficients are expressed in units of cm^3 molecule^{-1} s^{-1}. [b] Unreactive form of $C_3H_3^+$ (see text). [c] Generated by ionization of propyne. Assumed to have the propyne structure.

TABLE III: Branching Ratios for $C_4H_n^+$ Reactions in Pure Propyne

	ΔH°_{298}, kJ mol^{-1}
$C_4H_2^+ + C_3H_4 \xrightarrow{0.15} C_5H_4^+ + C_2H_2$	(−278)
$\xrightarrow{0.85} C_7H_5^+ + H$	(−476)
$C_4H_3^+ + C_3H_4 \xrightarrow{\geqslant 0.96} C_5H_5^+ + C_2H_2$	(−44)
$\xrightarrow{\leqslant 0.04} C_6H_5^+ + CH_2$	(268)
$C_4H_4^+ + C_3H_4 \xrightarrow{0.05} C_5H_6^+ + C_2H_2$	−227
$\xrightarrow{0.95} C_7H_7^+ + H$	−338
$C_4H_5^+ + C_3H_4 \xrightarrow{0.40} C_6H_5^+ + CH_4$	−107
$\xrightarrow{0.60} C_7H_7^+ + H_2$	−325
$C_4H_6^+ + C_3H_4 \xrightarrow{0.78} C_6H_7^+ + CH_3$	−186
$\xrightarrow{0.22} C_7H_9^+ + H$	−173

isomers of $C_3H_3^+$ are produced by electron impact of allene and propyne at 20 eV. The larger fraction of the $C_3H_3^+$ signal is the unreactive isomer, and it is this isomer that is included in Tables I and II listed as $C_3H_3^+$.. Double-resonance studies[20] of the reactive isomer of $C_3H_3^+$ gave the following products:

$$\begin{aligned}
C_3H_3^+ + \underset{\text{allene}}{H_2C{=}C{=}CH_2} &\xrightarrow{0.25} C_4H_3^+ + C_2H_4 \\
&\xrightarrow{0.37} C_4H_5^+ + C_2H_2 \\
&\xrightarrow{0.38} C_6H_5^+ + H_2 \\
C_3H_3^+ + \underset{\text{propyne}}{CH_3{-}C{\equiv}CH} &\xrightarrow{0.20} C_4H_3^+ + C_2H_4 \qquad (1) \\
&\xrightarrow{0.35} C_4H_5^+ + C_2H_2 \\
&\xrightarrow{0.45} C_6H_5^+ + H_2
\end{aligned}$$

The predominant reaction type for all the ion reactions studied is condensation with the subsequent loss of C_2H_2 or H. From

TABLE IV: Branching Ratios for $C_5H_n^+$ Reactions in Pure Propyne

	ΔH°_{298}, kJ mol^{-1}
$C_5H_3^+ + C_3H_4 \xrightarrow{0.81} C_6H_5^+ + C_2H_2$	−124
$\xrightarrow{0.19} C_8H_6^+ + H$	−106
$C_5H_4^+ + C_3H_4 \xrightarrow{0.57} C_6H_6^+ + C_2H_2$	(−118)
$\xrightarrow{0.43} C_8H_7^+ + H$	(−257)
$C_5H_5^+ + C_3H_4 \xrightarrow{0.56} C_6H_7^+ + C_2H_2$	−120
$\xrightarrow{0.44} C_8H_7^+ + H_2$	(−344)

TABLE V: Branching Ratios of Secondary and Tertiary Ions in Pure Propyne

	ΔH°_{298}, kJ mol^{-1}
$C_6H_5^{+\,a} + C_3H_4 \xrightarrow{0.2} C_7H_7^+ + C_2H_2$	−251
$\xrightarrow{0.7} C_9H_7^+ + H_2$	(−491)
$\xrightarrow{0.1} C_9H_8^+ + H$	−170
$C_6H_7^+ + C_3H_4 \xrightarrow{1.00} C_7H_7^+ + C_2H_4$	−117
$C_7H_7^+ + C_3H_4 \xrightarrow{0.10} C_9H_8^+ + CH_3$	47
$\xrightarrow{0.42} C_{10}H_9^+ + H_2$	−168
$\xrightarrow{0.48} C_{10}H_{11}^+ + h\nu$	(−328)
$C_9H_7^+ + C_3H_4 \longrightarrow C_{12}H_9^+ + H_2$	(−230)
$\longrightarrow C_{12}H_{11}^+ + h\nu$	(−315)

[a] Assumed to have the phenyl structure.

Tables I and II, it is evident that as the ions become more unsaturated (C_3H^+, $C_3H_2^+$), C_2H_2 loss is favored whereas the more saturated ion ($C_3H_4^+$) favors H loss. Each ion is seen to form the same products with both propyne and allene with the exception of an additional proton-transfer or hydrogen-abstraction channel between $C_3H_4^+$ and propyne to form the $C_3H_5^+$ product ion.

TABLE VI: Branching Ratios of Ions Generated by Electron Impact from the Source Gas Shown with Propyne

	ΔH°_{298}, kJ mol^{-1}
$C_4H_2^+$ (from diacetylene) + C_3H_4 $\xrightarrow{0.06}$ $C_5H_4^+ + C_2H_2$	(−278)
$\xrightarrow{0.94}$ $C_7H_5^+ + H$	(−467)
$C_4H_3^+$ (from vinylacetylene) + C_3H_4 $\longrightarrow$ $C_5H_5^+ + C_2H_2$[a]	(−44)
$\longrightarrow$ $C_6H_5^+ + CH_2$[a]	(268)
$C_4H_4^+$ (from vinylacetylene) + C_3H_4 $\longrightarrow$ $C_5H_6^+ + C_2H_2$[a]	−227
$\xrightarrow{>0.90}$ $C_7H_7^+ + H$[a]	−338[c]
$C_4H_5^+$ (from vinylacetylene) + C_3H_4 $\longrightarrow$ $C_6H_5^+ + CH_4$[a]	−107
$\longrightarrow$ $C_7H_7^+ + H_2$[a]	−325
$C_4H_6^+$ (from 1,3-butadiene) + C_3H_4 $\xrightarrow{0.90}$ $C_6H_7^+ + CH_3$	−186
$\xrightarrow{0.10}$ $C_7H_9^+ + H$	−173
$C_6H_5^+$ (from benzene) + C_3H_4 $\xrightarrow{0.24}$ $C_7H_7^+ + C_2H_2$	−251[c]
$\xrightarrow{0.67}$ $C_9H_7^+ + H_2$	(−491)
$\xrightarrow{0.09}$ $C_9H_8^+ + H$	−170
$C_7H_7^+$ (from toluene) + C_3H_4 $\xrightarrow{0.18}$ $C_8H_9^+ + C_2H_2$	4[b]
$\xrightarrow{0.18}$ $C_9H_7^+ + CH_4$	(−298)
$\xrightarrow{0.13}$ $C_9H_8^+ + CH_3$	22[b]
$\xrightarrow{0.20}$ $C_{10}H_9^+ + H_2$	−193
$\xrightarrow{0.31}$ $C_{10}H_{11}^+ + h\nu$	−353

[a] Branching ratio could not be determined. [b] Uncertainty in ΔH_f° is larger than the apparent endothermicity of this channel. [c] Calculated for the tropylium structure (see discussion).

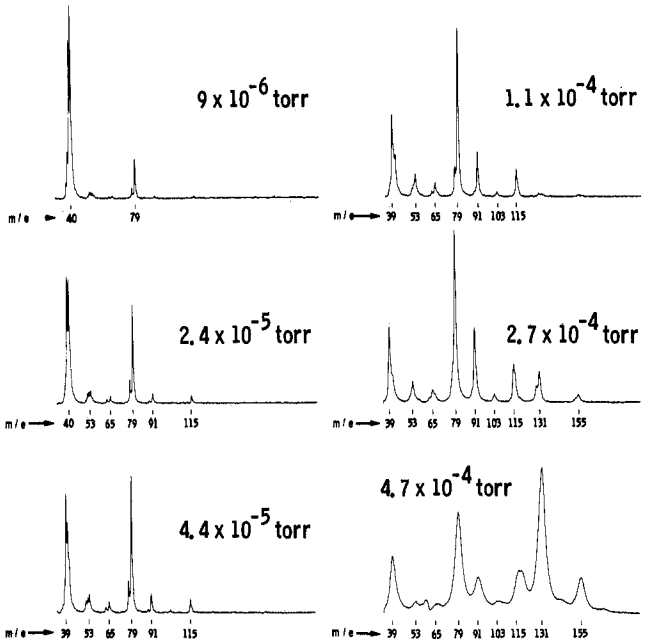

Figure 1. Six mass spectra of propyne at 30 eV. The propyne pressures are noted.

A study of the effect of pressure was made in the drit mode on both the allene and propyne systems. A similar result was obtained in each case. Figure 1 shows the results for the case of propyne subjected to 30-eV electron impact ionization. At a pressure of 9×10^{-6} torr the largest peaks are those of the parent ion $C_3H_4^+$ and the associated fragment ions arising from the ionization process. The fragment ions are not shown in Figure 1. The product peaks occur at m/e ratios of 50–54, 63, 65, 77, and 79. The products represent a 6% extent of reaction at 9×10^{-6} torr. The six different pressures in Figure 1 correspond to average numbers of collisions in the ICR cell, before detection, of 0.06, 0.16, 0.29, 0.72, 1.78, and >3.1. The initial reactant ions C_3H^+, $C_3H_2^+$, and $C_3H_4^+$ are depleted at the higher pressures and disappear when the pressure reaches 2.7×10^{-4} torr. New peaks appear at high pressures corresponding to secondary, tertiary, and higher order product ions at m/e 89, 91, 103, 115, 129, 131, and 155. The peaks at mass 129, 131, and 155 show that at least three consecutive reactions have occurred. It is also apparent that at higher pressures the $C_3H_3^+$ ion is unreactive ($k < 1 \times 10^{-11}$ cm^3 molecule^{-1} s^{-1}). The $C_6H_7^+$ ion at mass 79 and the $C_{10}H_{11}^+$ ion at mass 131 may have low reactivity as well.

The chemistry of the higher order hydrocarbon ions with propyne as listed in Tables III–VI was resolved by double-resonance experiments at higher pressures. Table III lists the branching ratios for reactions of $C_4H_n^+$ (n = 2–6) in propyne. Only condensation reactions are observed. Dissociation of the condensation product is mainly via C_2H_2 loss and via H loss for less saturated ions and via CH_3, CH_4, and H_2 loss for ions with $n \geq 5$. In Table IV we report the branching ratios for the reaction of $C_5H_n^+$ ions with propyne. The reactant ions in Table IV are secondary ions produced in the reactions shown in Tables II and III. Table V gives the branching ratios for reactions of several larger ions, which, as in the preceding table, are all products of earlier reactions. For example, double-resonance experiments demonstrated that the ion at m/e 155 ($C_{12}H_{11}^+$) originates from $C_3H_n^+$ in propyne by the following sequence of reactions:

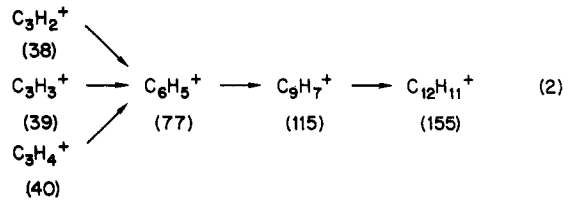

(2)

TABLE VII: $C_4H_n^+$ Reactions with Diacetylene[a]

	ΔH°_{298}, kJ mol^{-1}	$10^9 \times k_{exptl}$	$10^9 \times k_{ADO}$
$C_4^+ + C_4H_2 \longrightarrow C_8H^+ + H$	(−565)	1.7	1.4
$C_4H^+ + C_4H_2 \longrightarrow C_8H_2^+ + H$	(−465)	1.6	1.4
$C_4H_2^+ + C_4H_2 \xrightarrow{0.83} C_6H_2^+ + C_2H_2$	(−291)		
$\xrightarrow{0.17} C_8H_2^+ + H_2$	(−518)	1.4	1.4
$\xrightarrow{0.01} C_8H_3^+ + H$	(−620)		
$C_4H_3^+ + C_4H_2 \longrightarrow C_6H_3^+ + C_2H_2$	(−246)	0.74	1.4
$C_4H_4^+ + C_4H_2 \xrightarrow{0.87} C_6H_4^+ + C_2H_2$	−164		
$\xrightarrow{0.13} C_8H_6^+ + h\nu$	−524	0.80	1.4
$C_4H_5^+ + C_4H_2 \longrightarrow C_6H_5^+ + C_2H_2$	−93		1.4

[a] Rate coefficients are expressed in units of cm^3 molecule^{-1} s^{-1}.

Similarly, the $C_{10}H_9^+$ ion at mass 129 and the $C_{10}H_{11}^+$ ion at mass 131 were shown to arise from the reaction sequence

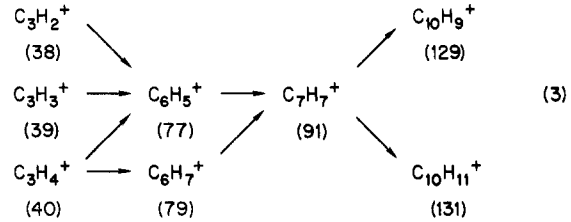

(3)

Structural isomerism is common in hydrocarbon ions. Although no direct evidence for the identification of isomers can be found from the results in this study, it is nevertheless possible in favorable cases to infer the existence of structural isomers from their differing reactivities. In an attempt to distinguish between different isomers, we generated a number of ions from sources other than propyne. Vinylacetylene was used as a source for $C_4H_3^+$ (51), $C_4H_4^+$ (52), and $C_4H_5^+$ (53), 1,3-butadiene for $C_4H_6^+$ (54), benzene for $C_6H_5^+$ (77), and $C_6H_6^+$ (78), and toluene for $C_7H_7^+$ (91). Table VI presents the branching ratios of the reactions of these ions with propyne. It is evident that, within experimental error, the product ratios are the same as for the equivalent ion formed in propyne. The sole exception is the $C_7H_7^+$ ion at mass 91, where $C_7H_7^+$ generated from toluene produced a markedly different distribution of products than $C_7H_7^+$ produced in reaction sequence (3).

Diacetylene and Vinylacetylene. Electron impact on diacetylene produces ions at m/e 48 (C_4^+), 49 (C_4H^+), and 50 ($C_4H_2^+$). Electron impact on vinylacetylene produces ions at m/e 50 ($C_4H_2^+$), 51 ($C_4H_3^+$), and 52 ($C_4H_4^+$). The $C_4H_5^+$ ion in pure vinylacetylene is the product of the reaction between $C_4H_3^+$ and C_4H_4. By analyzing the pure systems first and then mixtures of vinylacetylene and diacetylene, we identified the reactions of $C_4H_n^+$ (n = 0–5) ions with both gases. These results are reported in Table VII for diacetylene and in Table VIII for vinylacetylene. Each table lists the products and branching ratios, and total rate coefficient for all branches, the average-dipole-orientation (ADO) or Langevin collision rate,[26] and an estimate of the enthalpy change for each channel. The predominant reaction type is again condensation with subsequent loss of C_2H_2, H, or H_2. Charge-transfer channels were observed for reactions of C_4H^+ and $C_4H_2^+$ with vinylacetylene. At higher pressures (>10^{-5} torr), secondary reactions of $C_6H_n^+$ (n = 2–5) were observed, and branching ratios for these reactions are reported in Table IX. It is interesting to note that we have observed only one channel for each of the reactions of $C_6H_n^+$ we have studied, leading to the formation of $C_8H_n^+$ from C_4H_2 and $C_8H_{n+2}^+$ from C_4H_4.

Figure 2 shows the mass spectrum of a mixture of diacetylene and vinylacetylene. The inset in the figure gives the double-resonance spectrum of $C_6H_6^+$ obtained by observing the mass 78 peak while scanning the double-resonance oscillator over frequencies corresponding to m/e 46–55. The primary precursor of $C_6H_6^+$ is the $C_4H_4^+$ ion at mass 52:

$$C_4H_4^+ + C_4H_4 \rightarrow C_6H_6^+ + C_2H_2$$

The double-resonance signal coupling the mass 50 ion ($C_4H_4^+$) and the mass 78 product ion ($C_6H_6^+$) is not typical for a direct reaction. The primary reactions of $C_4H_2^+$ are

$$C_4H_2^+ + C_4H_2 \rightarrow C_6H_2^+ + C_2H_2$$

$$C_4H_2^+ + C_4H_4 \rightarrow C_6H_4^+ + C_2H_2$$

TABLE VIII: $C_4H_n^+$ Reactions with Vinylacetylene[a]

	ΔH°_{298}, kJ mol^{-1}	$10^9 \times k_{exptl}$	$10^9 \times k_{ADO}$
$C_4^+ + C_4H_4 \longrightarrow$ products		1.5	1.4
$C_4H^+ + C_4H_4 \xrightarrow{0.55} C_4H_4^+ + C_4H$	(−52)		
$\xrightarrow{0.37} C_6H_3^+ + C_2H_2$	(−603)	2.2	1.4
$\xrightarrow{0.08} C_8H_4^+ + H$	(−572)		
$C_4H_2^+ + C_4H_4 \xrightarrow{0.13} C_4H_4^+ + C_4H_2$	−58		
$\xrightarrow{0.80} C_6H_4^+ + C_2H_2$	−222		
$\xrightarrow{0.06} C_8H_4^+ + H_2$	(−625)	1.4	1.4
$\xrightarrow{\leq 0.01} C_8H_6^+ + h\nu$	−582		
$C_4H_3^+ + C_4H_4 \xrightarrow{0.25} C_4H_5^+ + C_4H_2$	(76)		
$\xrightarrow{0.65} C_6H_5^+ + C_2H_2$	(−17)	1.1	1.4
$\xrightarrow{0.10} C_8H_6^+ + H$	(1)		
$C_4H_4^+ + C_4H_4 \xrightarrow{0.38} C_6H_6^+ + C_2H_2$	−332		
$\xrightarrow{0.62} C_8H_7^+ + H$	(−471)	1.0	1.4
$C_4H_5^+ + C_4H_4 \longrightarrow C_6H_7^+ + C_2H_2$	−234		

[a] Rate coefficients are expressed in units of cm^3 molecule^{-1} s^{-1}.

TABLE IX: Higher Order Reactions of Secondary $C_6H_n^+$ Ions (n = 2–5) in Vinylacetylene and Diacetylene

	ΔH°_{298}, kJ mol^{-1}			
	n = 2	n = 3	n = 4	n = 5
$C_6H_n^+ + C_4H_2 \rightarrow C_8H_n^+ + C_2H_2$	(−246)	(−246)	(−422)	(−442)
$C_6H_n^+ + C_4H_4 \rightarrow C_8H_{n+2}^+ + C_2H_2$	(−353)	(−213)	−211	(−384)

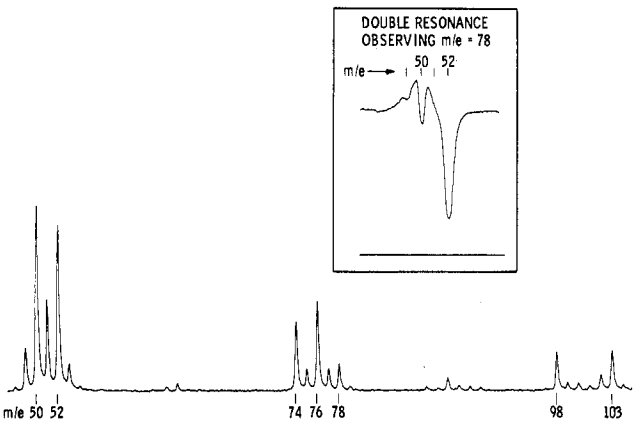

Figure 2. Mass spectrum of diacetylene/vinylacetylene mixture with diacetylene at 8 × 10^{-6} torr, vinylacetylene at 8 × 10^{-6} torr, and electron energy at 30 eV. The insert is the double-resonance spectrum of the m/e 78 ion showing the effects of ejecting the m/e 50 and 52 ions.

(26) W. J. Chesnavich, T. Su, and M. T. Bowers in "Kinetics of Ion–Molecule Reactions", P. Ausloos, Ed., Plenum Press, New York, 1979.

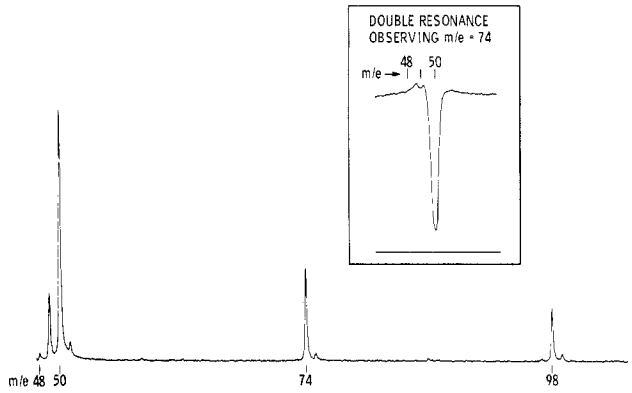

Figure 3. Mass spectrum of diacetylene at a pressure of 5×10^{-6} torr and electron energy at 30 eV. The insert is the double-resonance spectrum of the m/e 74 ion showing the effects of ejecting the m/e 48 and 50 ions.

Charge transfer from $C_4H_2^+$ to C_4H_4 is exothermic and it is this reaction

$$C_4H_2^+ + C_4H_4 \rightarrow C_4H_4^+ + C_4H_2 \quad (4)$$

that is responsible for the double-resonance signal shown in Figure 2. The occurrence of charge-transfer (4) was confirmed by examining a product of the reaction of the intermediate $C_4H_4^+$ ion with vinylacetylene other than $C_6H_6^+$. It is found that double resonance between $C_4H_2^+$ and $C_8H_7^+$ at mass 103 exhibits the same behavior as that presented for $C_6H_6^+$ in Figure 2.

Deconvoluton of the m/e 50 double-resonance signal from the double-resonance spectrum shown in Figure 2 results in a residual signal of m/e 49 due to the charge-transfer reaction

$$C_4H^+ + C_4H_4 \rightarrow C_4H_4^+ + C_4H \quad (5)$$

Reaction 5 accounts for 55% of the total reaction of C_4H^+ with vinylacetylene. A similar set of experiments was performed in pure diacetylene, and these are presented in Figure 3. The main product of C_4H^+ at mass 49 with diacetylene is $C_8H_2^+$ at mass 98. Charge transfer from C_4H^+ to diacetylene is exothermic, but the evidence for its occurrence was inconclusive. Double-resonance experiments to examine the secondary product of the charge-transfer reaction $C_4H^+ \rightarrow C_4H_2^+ \rightarrow C_6H_2^+$ at mass 74 did not indicate noticable chemical coupling (see inset, Figure 3). A similar result was obtained for the charge-transfer reaction of C_4^+ with diacetylene.

Thermochemistry

It is always desirable to have heats of formations available to determine which channels from a given pair of reactants are exothermic and which are endothermic. In the case of observed reactions, heats of formation can be used to determine if the observed reactions really are exothermic or endothermic channels being driven by excess energy in the reactants. The overall heat of reaction is used to select the most probable neutral products and also can be used to help specify a reaction mechanism.

A search of the available literature[27] shows that, of the more than 40 species observed in this work, just over half have heats of formation that were established to within a few kJ mol^{-1}. Unfortunately, very few data are available for unsaturated hydrocarbon ion containing more than three carbons. Table X contains all the literature values available for species observed in this study. In Table X we have noted specific ion structures where they are known and also have included several isomeric structures where information was available. Without all the necessary heats of formation the question can be asked, what can we do with the existing literature to help determine the thermochemistry of the reactions observed in this work?

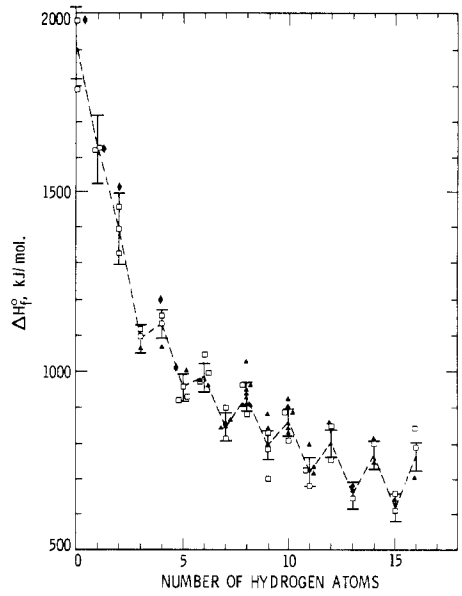

Figure 4. A plot of the ΔH_f° values of selected hydrocarbon ions according to the number of hydrogen atoms in their formula. Error bars are used to note estimated heats of formation used in Table XI. The dashed line shows the trends of ΔH_f° with the number of hydrogen atoms. Cyclic structures are noted by ▲. Alicyclic structures are noted by □. Where the structure is known ♦ is used.

The first task is to decide on the series of available exit channels. Each exit channel may have several possible structural isomers for each product. To determine, to a first approximation, if a pair of reactants will form a new product pair, we can look at just the lowest energy isomer available for the products. This does not take into account possible barriers to rearrangement. Most ion structures are inferred from the structure of their neutral source and by comparison with MINDO type calculations. Standard techniques used for determining the structure of neutral species (e.g. X-ray defraction, NMR spectropscopy, etc.) are not applicable for the small abundances of ions produced in the laboratory. Table X notes several assumed structures, but generally the ions are assumed to have the same structure as their parent neutrals. This assumption is known to be false in a few instances. It has therefore been necessary to approximate the heats of formation of some of the hydrocarbon ions. These ions contain more than four carbons and therefore have several possible isomeric structures. The present survey of heats of formation shows that in some cases lowest energy isomers are linear or alicyclic and in other cases they are cyclic. We have used a group equivalent type method is to estimate lower limits for these unknown heats of formation. These estimates are applied only to the lowest energy isomers.

The group equivalents method[27a,28] is a technique of correlating changes of the heats of formation with changes in the chemical structure. This can consist of additions of CH_2 to a carbon chain, substitutions of fluorine for hydrogen in a structure, etc. In our attempts we have tried to correlate various aspects of the hydrocarbon ion structure with their heats of formation. An analysis of all known tabulated heats of formation[27-33] of hydrocarbon ions

(27) (a) J. L. Franklin, J. G. Dillard, H. M. Rosenstock, J. T. Herron, and K. Draxl, *Natl. Stand. Ref. Data Ser. (U.S., Nat. Bur. Stand.)*, **NSRDS-NBS 26** (1969); (b) H. . Rosenstock, K. Draxl, B. W. Steiner, and J. T. Herron, *J. Phys. Chem. Ref. Data*, **6** (1977).

(28) J. L. Holmes, F. Fingas, and F. P. Lossing, *Can. J. Chem.*, **59**, 80 (1981).

(29) M. Cowperthwaite and S. H. Bauer, *J. Chem. Phys.*, **36**, 1743 (1962) (estimated values).

(30) D. R. Stull, E. F. Westrum, and G. C. Sinke, "The Chemical Thermodynamics of Organic Compounds," Wiley, New York, 1969.

(31) H. M. Rosenstock and K. E. McCulloh, *Int. J. Mass Spectrom. Ion Phys.*, **25**, 327 (1977); R. Stockbauer and H. M. Rosenstock, *Int. J. Mass Spectrom. Ion Phys.*, **27**, 185 (1978); A. C. Parr, A. J. Jason, R. Stockbauer, and K. E. McCulloh, *Int. J. Mass Spectrom. Ion Phys.*, **30**, 319 (1979).

(32) C. Lifshitz, D. Gibson, K. Levsen, and I. Dotan, *Int. J. Mass Spectrom. Ion Phys.*, **40**, 157 (1981).

(33) Calculated from proton affinities listed by K. N. Hartman, S. Lias, P. Ausloos, H. M. Rosenstock, S. S. Schroyer, C. Schmidt, D. Martinsen, and G. W. A. Milne, *Nat. Bur. Stand.*, [*Tech. Rep.*] *NBSIR (U.S.)*, **NBSIR-79-1777** (1979).

TABLE X: Heats of Formation of Reactants and Products ($\Delta H_f°_{298}$(g), kJ mol^{-1})

formula		$\Delta H°$	ref	formula		$\Delta H°$	ref
H	atomic hydrogen	218	*a*	$C_4H_{10}^+$	isobutane	≤879	*a*
CH_2	methylene	392	*a*	$C_4H_{11}^+$	protonated butane	711	*e*
CH_3	methyl	142	*a*	$C_5H_3^+$	1,3-pentadiyne	1317	*j*
CH_4	methane	−74.8	*a*	$C_5H_5^+$	cyclopentadienyl	~1004	*k*
C_2H_2	acetylene	227	*a*	$C_5H_5^+$	3-penten-1-yne	~1159	*l*
C_2H_3	vinyl	~280	*b*	$C_5H_6^+$	cyclopentadiene	960	*a*
C_2H_4	ethylene	52.3	*a*	$C_5H_7^+$	cyclopentenyl	833	*d, i*
C_3H_3		338	*a*	$C_5H_8^+$	cyclopentene	902	*a*
C_3H_4	propyne	185.4	*a*	$C_5H_9^+$	2-pentenyl	768	*d*
C_3H_4	allene	192.1	*a*	$C_5H_{10}^+$	2-methyl-2-butene	795	*a*
C_4		~998	*b*	$C_5H_{11}^+$	2-methylbutyl	665	*d*
C_4H		~644	*b*	$C_5H_{12}^+$	neopentane	≤835	*a*
C_4H_2	butadiyne	473	*a*	$C_6H_4^+$	benzyne	1311	*m*
C_4H_4	vinylacetylene	305	*c*	$C_6H_4^+$	3-hexen-1,5-dyne	1403	*m*
C^+	carbon	1797.6	*a*	$C_6H_5^+$	phenyl	1151	*g*
CH^+	methylidyne	1619	*a*	$C_6H_5^+$	alicyclic?	1176	*g*
CH_2^+	methylene	~1398	*a*	$C_6H_6^+$	benzene	975	*a*
CH_3^+	methyl	1092	*d*	$C_6H_7^+$	cyclohexadienyl	842	*d*
CH_4^+	methane	≤1150	*a*	$C_6H_8^+$	1,3-cyclohexadiene	904	*a*
CH_5^+	protonated methane	912	*e*	$C_6H_{10}^+$	1-methyl-cyclopentene	819	*a*
C_2^+		1992	*a*	$C_6H_{11}^+$	1-methyl-cyclopentyl	703	*d*
C_2H^+	ethynyl	1632	*f*	$C_6H_{12}^+$	2,3-dimethyl-2-butene	742	*a*
$C_2H_2^+$	acetylene	1328	*a*	$C_6H_{13}^+$	2,3-dimethyl-2-butyl	629	*d*
$C_2H_3^+$	vinyl	1113	*d*	$C_6H_{14}^+$	2,2-dimethylbutane	≤785	*a*
$C_2H_4^+$	ethylene	1075	*a*	$C_7H_7^+$	tropylium	~858	*n*
$C_2H_5^+$	ethyl	~917	*a, e*	$C_7H_7^+$	benzyl	~883	*o*
$C_2H_6^+$	ethane	~1041	*a*	$C_7H_8^+$	toluene	901	*a*
$C_2H_7^+$	protonated ethane	888	*e*	$C_7H_9^+$	methylcyclohexadienyl	779	*d*
C_3^+		~1988	*a*	$C_7H_{12}^+$	*cis*-cycloheptane	847	*a*
C_3H^+		1620	*g*	$C_7H_{13}^+$	methylcyclohexyl	657	*d*
$C_3H_2^+$		1507	*g*	$C_7H_{14}^+$	methylcyclohexane	796	*a*
$C_3H_3^+$	cyclopropenyl	1071	*a, d, h*	$C_7H_{15}^+$	2,2,3-trimethylbutyl	593	*d*
$C_3H_3^+$	propargyl	1177	*a, d, h*	$C_7H_{16}^+$	*n*-heptane	~776	*a*
$C_3H_4^+$	allene	~1124	*a*	$C_8H_6^+$	ethynylbenzene	1178	*a*
$C_3H_4^+$	propyne	1185	*a*	$C_8H_8^+$	ethenylbenzene	962	*a*
$C_3H_4^+$	*cis*-cyclopropene	~1209	*a*	$C_8H_9^+$	ethylbenzene	845	*d, e, n*
$C_3H_5^+$	allyl	946	*a*	$C_8H_{10}^+$	*p*-xylene	834	*a*
$C_3H_5^+$	propenyl	962	*d*	$C_8H_{11}^+$	dimethylcyclohexadienyl	721	*d*
$C_3H_5^+$	cyclopropyl	983	*d*	$C_8H_{15}^+$	2,3,4-trimethyl-2-pentenyl	644	*d*
$C_3H_6^+$	propene	960	*a*	$C_8H_{16}^+$	1-octene	827	*a*
$C_3H_7^+$	isopropyl	783	*d*	$C_9H_8^+$	indene	948	*a*
$C_3H_8^+$	propane	≤953	*a*	$C_9H_{10}^+$	isopropenylbenzene	917	*a*
$C_3H_9^+$	protonated propane	816	*e*	$C_9H_{11}^+$	isopropylbenzene	787	*d, e*
$C_4H_2^+$	butadiyne	1455	*a*	$C_9H_{12}^+$	1,2,4-trimethylbenzene	784	*a*
$C_4H_4^+$		~1192	*g*	$C_9H_{13}^+$	1,3,5-trimethyl-1,3-cyclohexadienyl	672	*d*
$C_4H_4^+$	vinylacetylene	1229	*g*	$C_{10}H_8^+$	naphthalene	936	*a*
$C_4H_5^+$		998	*a, i*	$C_{10}H_9^+$	protonated azulene	875	*e*
$C_4H_6^+$	*trans*-1,3-butadiene	985	*a*	$C_{10}H_{14}^+$	1,2,4,5-tetramethylbenzene	730	*a*
$C_4H_6^+$	cyclobutene	1040	*a*	$C_{10}H_{15}^+$	2,4,4-trimethyl-1-cyclohezenyl	624	*d*
$C_4H_6^+$	1,2-butadiene	1053	*a*	$C_{11}H_{10}^+$	2-methylnaphthalene	884	*a*
$C_4H_6^+$	2-butyne	1069	*a*	$C_{11}H_{16}^+$	pentamethylbenzene	690	*a*
$C_4H_7^+$	1-butenyl	837	*d*	$C_{12}H_8^+$	acenaphthylene	1032	*a*
$C_4H_8^+$	isobutene	~871	*a*	$C_{12}H_{10}^+$	acenaphthene	902	*a*
$C_4H_9^+$	*tert*-butyl	686	*d*	$C_{16}H_{10}^+$	fluoranthene	1047	*a*

[a] See ref 27. [b] See ref 29. [c] See ref 30. [d] D. H. Aue and M. T. Bowers, "Gas Phase Ion Chemistry", Vol. 2, M. T. Bowers, Ed., Academic Press, New York, 1979, p 1. [e] Calculated from ref 33. [f] Y. Ono and C. Y. Ng, *J. Chem. Phys.*, **74**, 6985 (1981). [g] See ref 31. [h] J. L. Holmes and F. P. Lossing, *Can. J. Chem.*, **57**, 249 (1979). [i] J. L. Holmes, *Org. Mass Spectrom.*, **8**, 247 (1974). [j] J. Dannacher, E. Heilbronner, J. P. Stadelmann, and J. Vogt, *Helv. Chim. Acta*, **62**, 2186 (1979). [k] P. F. Pottie and F. P. Lossing, *J. Am. Chem. Soc.*, **85**, 269 (1963). [m] H. M. Rosenstock, R. Stockbauer, and A. C. Parr, *J. Chim. Phys. Phys.-Chim. Biol.*, **77**, 745 (1980). [n] See ref 49. [o] F. A. Houle and J. L. Beauchamp, *J. Am. Chem. Soc.*, **100**, 3290 (1978).

results in 123 values for specific formulas, some of which can be associated with a specific structural isomer. Table X is only a partial listing of this tabulation. Eliminating all but the most stable isomers reduces this set to 76 heats of formation. We have found a simple approach which shows an interesting correlation of $\Delta H_f°$ with the number of hydrogen atoms. Figure 4 shows this correlation. There is a sharp reduction of the heats formation with the addition of the first three hydrogen atoms. After the last three there is a slower oscillatory behavior which has a shallower rate of reduction. The behavior of the $\Delta H_f°$ with the number of carbon atoms seems to be random. This randomness was used to get the error bars on the estimated values. Table XI lists the extimated heats of formation of the most stable isomers with error bar estimations. These may be considered lower limits for all isomeric forms of these ions. Tables I–IX include the calculated heats of reaction. Tabulated values of $\Delta H_f°$ are taken from Table X when they are available, and estimated values of the heats of formation from Table XI are used otherwise. If estimated values are used, the heats of reactions on Table I–IX are bracketed.

Discussion

Comparison with Other Measurements. Three different techniques have been used to study the ion chemistry of the systems reported here. Bowers et al.[4] used the ICR technique and reported branching ratios for reactions of $C_3H_4^+$ that are identical (within experimental error) with this work for both allene and propyne. Trapped-ion mass spectrometry has been applied by two groups: Myher and Harrison in 1968[1] and more recently Lifshitz et al.[2]

TABLE XI: Estimated Heats of Formation (in kJ mol^{-1}) of Lowest Energy Isomer of Hydrocarbon Ions[a]

formula	value	uncertainty
C_n^+	1930	100
C_nH^+	1620	45
$C_nH_2^+$	1410	100
$C_nH_3^+$	1090	45
$C_nH_4^+$	1135	45
$C_nH_5^+$	955	45
$C_nH_6^+$	985	45
$C_nH_7^+$	845	45
$C_nH_8^+$	935	45
$C_nH_9^+$	800	45
$C_nH_{10}^+$	860	45
$C_nH_{11}^+$	715	45
$C_nH_{12}^+$	800	45
$C_nH_{13}^+$	653	45
$C_nH_{14}^+$	770	45
$C_nH_{15}^+$	620	45
$C_nH_{16}^+$	764	45

[a] No specific structure is assumed (see text).

Finally, Lifshitz et al.[2,3] and Nato et al.[34] have applied photoionization mass spectrometry techniques. Each of these groups examined reactions for the $C_3H_4^+$ ion from both allene and propyne. Their results are compared with the present work in Table XII. The channel leading to $C_3H_3^+$ in the reaction of $C_3H_4^+$ with allene and propyne was not observed in the present ICR measurements but was prepared as a 16% channel in allene and a 17% channel in propyne in the photoionization work of Nato et al.[34] Nato et al. used a 10.2-eV Lyman α source and observed an initial primary production of $C_3H_3^+$ which may have originated from the Penning reaction (6). $C_3H_3^+$ cannot be formed directly

$$C_3H_4 + h\nu \rightarrow C_3H_4^* + C_3H_4 \rightarrow C_3H_3^+ + C_3H_5 + e \quad (6)$$

by dissociative photoionization with 10.2-eV photons. Lifshitz and Gleitman[3] also suggest Penning ionization to be responsible for the initial $C_3H_3^+$ observed in their photoionization experiments at photon energies below the ionization threshold of allene. Because this Penning ionization is pressure dependent, it is difficult to obtain branching ratios for $C_3H_3^+$ from photoionization experiments of allene. A further difficulty inherent in studies of $C_3H_4^+$ reactions is in the identification of the structural isomer. There are three isomers of $C_3H_4^+$: an allene ion structure $CH_2{=}C{=}CH_2^+$ (ΔH_f° = 1124 kJ mol^{-1}), a propyne ion structure $CH_3{-}C{\equiv}CH^+$ (ΔH_f° = 1184 kJ mol^{-1}), and a cyclic structure ($\Delta H_f^\circ \sim$ 1209 kJ mol^{-1}).[31] Photodissociation studies of $C_3H_4^+$ have distinguished between $CH_2{=}C{=}CH_2^+$ and $CH_3{-}C{\equiv}CH^+$ and have shown that when propyne is subjected to 12–16-eV electron impact, about 14% of the $CH_3{-}C{\equiv}CH^+$ ions revert to the allene structure in the time scale of an ICR experiments.[35] Thus, we expect $C_3H_4^+$ from allene in our work to be $H_2C{=}C{=}CH_2^+$ and $C_3H_4^+$ from propyne to be mainly the $H_3C{-}C{\equiv}CH^+$ structure. Nato et al., however, generated $C_3H_4^+$ in mixtures of allene and propyne at photon energies below the ionization potential of propyne. Therefore, the $C_3H_4^+$ ion in their study should have the $H_2C{=}C{=}CH_2^+$ structure only. These differences in ion structure clearly influence the product distributions as the different structures donate different amounts of energy to the activated intermediate. The agreement shown in Table XII among different laboratories (with the exception of the $C_3H_3^+$ channel in the work of Nato et al.[34]) is thus surprisingly good. Evidence gathered to date supports a mechanism for the reaction whereby condensation via a "tight" complex $(C_6H_8^+)^*$ is in competition with the channels leading to $C_3H_5^+$ and $C_3H_3^+$ that are formed directly from the "loose" complex $(C_3H_4{\cdot}C_3H_4)$.[1,2] The much greater production of $C_3H_5^+$ in propyne from $H_3C{-}C{\equiv}CH^+$ compared with the case of $H_2C{=}C{=}CH_2^+$ on allene (see Table XII) is therefore a consequence of the greater energy input of $H_3C{-}C{\equiv}CH^+$ into the loose complex. Nato et al., using only the $H_2C{=}C{=}CH_2^+$ structure, did not distinguish any difference in the $C_3H_5^+$ branching ratio between allene and propyne. It is not known whether $C_3H_5^+$ is the result of proton transfer from $C_3H_4^+$ to C_3H_4 or H abstraction from C_3H_4 by $C_3H_4^+$.

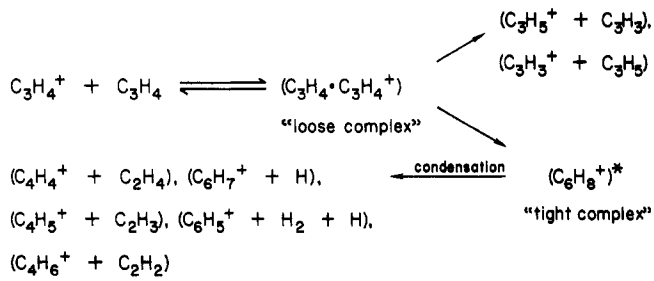

Condensation Reactions. In the four unsaturated hydrocarbon systems investigated, over 90% of the reactive channels lead to product ions containing more carbon atoms than the reactant ion. No clear trend in the product distributions seems to account for the majority of product ions observed. In allene and propyne, the most unsaturated ion in the $C_3H_n^+$ series reacts to give a single product ion plus H, but with $n > 1$ two or more product ions are produced. A similar trend is observed in the reaction series $C_2H_n^+ + C_2H_2$ where a single product ion plus H is found for $n = 0$ or 1.[10-19,36]

An attempt can be made to rationalize the distribution of products by considering how the internal energy within each intermediate complex might be distributed. For example, in the reactions between $C_4H_4^+$ and C_4H_2 (Table VII) and between $C_4H_2^+$ and C_4H_4 (Table VIII), a condensation adduct ion ($C_8H_6^+$) is observed in each reaction. The $(C_8H_6^+)^*$ ion may be stabilized by collisional or radiative processes, or alternatively the ion may undergo one of several possible dissociative processes. In addition to condensation, charge transfer proceeds as an independent channel in the $C_4H_2^+/C_4H_4$ system. We have observed the $C_8H_6^+$ product ion in both systems at pressures as low as 1×10^{-6} torr and have also found the rate coefficients to be independent of pressure. These observations indicate that $C_8H_6^+$ is formed in a bimolecular reaction and not by collisional stabilization. Lifetimes for these condensation complexes must exceed 2 ms in order to be observed in our system, which exceeds the lifetime of any unstabilized ion–molecule association complex. We have therefore assumed the $(C_8H_6^+)^*$ intermediate to be stabilized by rapid radiative processes and have indicated radiative stabilization by photon emission in those product channels where the parent condensation ion is observed. For radiative stabilization to occur, the potential energy surface entered by the reactant species must have a potential well with a sufficient density of energy levels to trap the unstabilized complex long enough for it to lose internal energy. The lifetime for an electronic transition is typically $<10^{-5}$–10^{-6} s and for a vibrational transition $\sim 10^{-2}$–10^{-3} s. At the total energies of these reactions a number of different isomeric ions are energetically accessible. Unfortunately, the structural isomers of $C_8H_6^+$ have not been well characterized, but it appears the most stable is the ethynylbenzene ion $Ph{-}C^+{\equiv}C{-}H$[37] (ΔH_f° = 1178 kJ mol^{-1}), and if this is the isomer we observe, then up to 580 kJ mol^{-1} of internal energy must be dissipated. It is not necessary for all of this energy to be lost by photon emission. The fragmentation channels observed for $(C_8H_6^+)$ are

$$(C_8H_6^+)^* \rightarrow C_8H_4^+ + H_2 \quad \text{(from } C_4H_2^+/C_4H_4 \text{ only)}$$

$$\rightarrow C_6H_4^+ + C_2H_2 \quad \text{(from } C_4H_2^+/C_4H_4 \text{ and } C_4H_4^+/C_4H_2\text{)}$$

Neither of these ions, $C_8H_4^+$ nor $C_6H_4^+$, are likely unimolecular dissociation fragments of $(Ph{-}C^+{\equiv}C{-}H)^*$ but are likely fragments from alicyclic isomer precursors such as (H—C≡

(34) A. Nato, M. Niwa, K. Honma, and I. Tanaka, *Int. J. Mass Spectrom. Ion Phys.*, **34**, 287 (1980).
(35) P. N. T. Van Velzen and W. J. Van der Hart, *Org. Mass Spectrom.*, **16**, 237 (1981).
(36) W. T. Huntress, *Astrophys. J., Suppl. Ser.*, , **33**, 495 (1977).
(37) J. L. Franklin and S. R. Carroll, *J. Am. Chem. Soc.*, , **91**, 5940 (1969).

TABLE XII: Comparison of Branching Ratios for Fractions of $C_3H_4^+$ with Allene and Propyne

	allene					propyne			
product ion	this work	ref 4	ref 1	ref 3[a]	ref 34[b]	this work	ref 4	ref 1	ref 34[b]
$C_3H_3^+$			0.01	≤0.03	0.16			0.03	0.17
$C_3H_5^+$		0.04	0.06	≤0.03	0.11	0.18	0.17	0.34	0.11
$C_4H_3^+$				trace					
$C_4H_4^+$	0.05	0.06	0.10	0.05		0.02	0.04	0.06	
$C_4H_5^+$				trace					
$C_4H_6^+$	0.01		0.01	trace		0.02	0.04	0.04	
$C_5H_5^+$	0.01	0.03	0.02	trace		0.02	0.04	0.06	
$C_6H_5^+$	0.07	0.04	0.02	trace	0.01	0.08	0.06	0.02	0.01
$C_6H_6^+$		0.01					0.01		
$C_6H_7^+$	0.87	0.81	0.76	≥0.90	0.72	0.68	0.66	0.45	0.71

[a] $C_3H_4^+$ ion derived from 9.7–10.8-eV photoionization of allene (ref 3). [b] $C_3H_4^+$ ion derived from 10.2-eV photoionization of allene.

TABLE XIII: A Comparison of Rate Coefficients of the Ions Shown with Allene, Propyne, and Vinylacetylene (1-Buten-3-yne)

	allene				
reactant ion	this work	ref 1	ref 2	ref 34	ADO
C_3H^+	1.4		1.0[a]		1.3
$C_3H_2^+$	1.4		1.2[a]		1.3
$C_3H_3^+$	≤0.01				1.3
$C_3H_4^+$	1.1	0.6	0.6	1.1	1.3

	propyne				
reactant ion	this work	ref 1	ref 2	ref 34	ADO
C_3H^+	1.4		1.1[a]		1.3
$C_3H_2^+$	1.3		1.2[a]		1.3
$C_3H_3^+$	≤0.01				1.3
$C_3H_4^+$	1.1	1.6	1.5	1.1	1.3

	vinylacetylene			
reactant ion	this work	ref 31[b]	ref 31[c]	ADO
C_4H^+	2.2	1.3		1.4
$C_4H_2^+$	1.4	1.0		1.4
$C_4H_3^+$	1.1	0.47		1.4
$C_4H_4^+$	1.0	0.58	0.9	1.4

[a] Nominal electron energy 32 eV. [b] Nominal electron energy 50 eV. [c] Nominal electron energy 15 eV.

C—CH=CH—CH=CH—C^+≡C—H)* or perhaps an alternative cyclic isomer benzocyclobutadiene[38] (Ph-c-Bu). A possible mechanism for the $C_4H_2^+/C_4H_4$ and $C_4H_4^+/C_4H_2$ reactions is thus formation of an initial alicyclic intermediate, such as (HC≡C—C=CH—CH_2—CH^+—C=CH)*, which interconverts to other isomers from which dissociation occurs with loss of H_2 or C_2H_2. If during the interconversion, a particularly stable isomer is encountered (possibly the ethynylbenzene structure) leading to a high density of states, radiative stabilization may occur.

Hydride transfer has been observed previously as a minor channel in the reactions of C^+ with unsaturated hydrocarbons including allene.[39] Careful double-resonance experiments were performed to determine if hydride transfer reactions were occurring in the reactions studied in this work. None were detected, and an upper limit of the possible branching ratios was set at 5–10%. Where the hydride-transfer reaction is symmetric, i.e., reactant and product ions are identical as in $C_3H_3^+ + C_3H_4 \rightarrow C_3H_4 + C_3H_3^+$, no upper limit could be set. Two other potential symmetric hydride-transfer reactions are $C_4H^+ + C_4H_2 \rightarrow C_4H_2 + C_4H^+$ and $C_4H_3^+ + C_4H_4 \rightarrow C_4H_4 + C_4H_3^+$. These reactions would also escape detection.

Structural Isomerism. The majority of cations observed in this work have several possible structural isomers. For example, two isomers of C_3H^+ are possible: a linear :C—C=C^+—H structure and a nonlinear structure

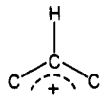

both of which are stabilized by charge delocalization. The nonlinear structure has been calculated to be higher in energy by ~190 kJ mol^{-1} [40] and is therefore not favored as the isomer produced by electron impact on allene and propyne.

The existence of stable isomers for $C_3H_3^+$ has been well documented.[41] On the basis of this earlier work, we assume that both the cyclopropenium ion and the propargyl ion are produced by electron impact on allene and propyne and that the reactive fraction of $C_3H_3^+$ ions in allene and propyne is the fraction with the higher energy propargyl structure H_2C—C=C^+H.

Two different alicyclic structures have been observed for the $C_3H_4^+$ ion, and these have been discussed briefly in a preceding section. The ion derived from allene, H_2C—C=C^+H. Photodissociation studies of these ions led to the conclusion that $C_3H_4^+$ produced by electron impact on allene is H_2C—C^+=H_2 and that $C_3H_4^+$ produced by electron impact on propyne is mainly H_3C—C=C^+H.[35] The $C_3H_4^+$ ions produced by these processes in our experiments react at essentially every collision and show little difference in reactivity in the systems studied.

A similar situation may also exist with the $C_4H_2^+$ ion derived from electron impact on diacetylene, HC=C—C=C^+H, and vinylacetylene, H_2C=C=C=C^+·, although the most stable geometry corresponds to the diacetylene structure. The $C_4H_2^+$ ions produced by either method were found to have the same reactive properties.

A number of isomers have been proposed for $C_4H_4^+$ produced by electron impact on vinylacetylene, benzene, and pyridine. One $C_4H_4^+$ isomer derived from benzene and pyridine was found to have an energy 29–75 kJ mol^{-1} lower than the linear isomer H_2C=CH—C≡CH derived from vinylacetylene.[30,42] A cyclic structure, either the cyclobutadiene radical cation or the methylene cyclopropene cation,[43,44] is favored for the more stable $C_4H_4^+$ isomer produced by unimolecular decomposition of excited $C_6H_6^+$. Ausloos[43] was able to distinguished between two isomeric forms of $C_4H_4^+$ on the basis of their different reactivity with benzene: one isomer was found to be reactive and the other nonreactive. Wanger-Redeker et al.[45] have noted that $C_4H_4^+$ has a similar behavior in reactions with acetylene. Ausloos showed that the

(38) T. Koenig, D. Imre, and J. A. Hoobler, *J. Am. Chem. Soc.*, **101**, 6446 (1979).
(39) D. K. Bohme,,A. B. Bakshit, and H. I. Schiff, *Chem. Phys. Lett.*, **93**, 592 (1982).
(40) L. Radom, P. C. Hariharan, J. A. Pople, and P. V. R. Schleyer, *J. Am. Chem. Soc.*, **98**, 10 (1976).
(41) P. J. Ausloos and S. G. Lias, *J. Am. Chem. Soc.*, **103**, 6505 (1981).
(42) H. M. Rosenstock, R. Stockbauer, and A. C. Parr, *Int. J. Mass Spectrom. Ion Phys.*, **38**, 323 (1981).
(43) P. Ausloos, *J. Am. Chem. Soc.*, , **103**, 3931 (1981).
(44) T. Baer, G. D. Willett, D. Smith, and J. S. *Phillips, J. Chem. Phys.*, **70**, 4076 (1979).
(45) W. Wagner-Redeker, A. J. Illies, P. R. Kemper, and M. T. Bowers, *J. Am. Chem. Soc.*, in press.

reactive isomer has the same behavior when produced from 1,5-hexadiyne, 2,4-hexadiyne, and pyridine and concluded that reactive $C_4H_4^+$ has the vinylacetylene structure. We assume the $C_4H_4^+$ reactant ion produced by electronimpact on vinylacetylene in our study has the vinylacetylene structure. The $C_4H_4^+$ ions produced in the reactions studied may have cyclic, linear, or a mixture of both structures.

Several isomeric forms may be written for $C_6H_7^+$. Experimental evidence indicates that both alicyclic and cyclic structures are stable, but with the cyclic structure having a heat of formation lower by 190 kJ mol^{-1}.[3] Collisional activation spectra of various $C_6H_7^+$ ions support the idea that the $C_6H_7^+$ isomer produced via secondary reaction in both allene and propyne had mainly the cyclic benzenium ion structure[46,47]

We have found in this study that the major fraction of the $C_6H_7^+$ formed in allene and propyne (Tables I and II) is unreactive. The small fraction that does react gives $C_7H_7^+$ and C_2H_4 as products (reaction 7, see Table V). In addition, electron impact on 1,3-

$$\underset{\text{propyne}}{C_6H_7^+ + C_3H_4} \rightarrow C_7H_7^+ + C_2H_4 \qquad (7)$$

butadiene produced a $C_4H_6^+$ ion which reacts with propyne to form a reactive $C_6H_7^+$ structure.

$$C_4H_6^+ + C_3H_4 \rightarrow C_6H_7^+ + CH_3$$

This reactive $C_6H_7^+$ isomer reacts with propyne to produce the same products as in reaction 7. We therefore conclude that the $C_6H_7^+$ species produced in ion–molecule reactions of allene and propyne has two components: as alicyclic reactive structure (minor fraction) and a cyclic unreactive structure, presumably the cyclic benzenium structure (major fraction).

The difference in reactivity previously reported between $C_7H_7^+$ produced from toluene and $C_7H_7^+$ produced in reaction sequence (2) may also be due to structural isomerism. ICR studies of $C_7H_7^+$ produced by photoionization of toluene have shown that both reactive and unreactive isomers are formed.[48] The less reactive isomer was attributed to the tropylium structure and the more reactive form to the benzyl structure. These two structures differ

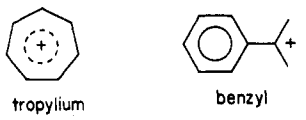

in their heats of formation by at least 22 kJ mol^{-1}.[49] Presumably, in our work the $C_7H_7^+$ produced via reaction sequence (2) has the benzyl ion structure because of its demonstrated reactivity.

Acknowledgment. This paper presents the results of one phase of research carried out at the Jet Propulsion Laboratory, California Institute of Technology, under Contract No. NAS 7-918, sponsored by the National Aeronautics and Space Administration.

Registry No. Allene, 463-49-0; propyne, 74-99-7; diacetylene, 460-12-8; vinylacetylene, 689-97-4.

(46) R. Wolfschutz, H. Schwartz, and K. Levsen, unpublished results quoted in ref 3.
(47) C. Lifshitz and Y. Gleitman, *J. Chem. Phys.*, **77**, 2383 (1982).
(48) R. C. Dunbar, *J. Am. Chem. Soc.*, **97**, 1382 (1975); J. L. M. Abboud, W. J. Hehre, and R. W. Taft, *J. Am. Chem. Soc.*, **98**, 6072 (1976).
(49) R. G. McLoughlin, J. D. Morrison, and J. C. Traeger, *Org. Mass Spectrom.*, **14**, 104 (1979).

Theoretical Investigation of the Addition of Molecular Hydrogen to Pd and $(H_2O)_2Pd$

Ulf B. Brandemark,* Margareta R. A. Blomberg, Lars G. M. Pettersson, and Per E. M. Siegbahn

Institute of Theoretical Physics, University of Stockholm, Vanadisvägen 9, S-113 46 Stockholm, Sweden
(Received: August 22, 1983)

The concerted oxidative addition of molecular hydrogen to the naked palladium atom and to the complex $(H_2O)_2Pd$ is studied by using multireference CI calculations. It is found that stable complexes are formed in both cases with binding energies of about 5 kcal/mol. The equilibrium geometries are rather different, however, and also the character of the bonding. The interaction of the d^{10} ground state of the palladium atom with molecular hydrogen causes only a slight increase of the H–H bond distance and the Pd–H bonding is hardly reflected in the wave function. The addition of water ligands to Pd lowers the atomic d^9s configuration relative to the ground state and thus facilitates sd hybridization. This results in the formation of covalent Pd–H bonds and the complete splitting of the H–H bond in $(H_2O)_2PdH_2$. The metal–hydrogen bonding in *cis*-$(H_2O)_2PdH_2$ is very similar to that obtained without extra ligands in NiH_2.

Introduction

Hydrogenation, the addition of molecular hydrogen to an unsaturated system, e.g., an olefin, is an important reaction that is catalyzed by transition metals. Homogeneous hydrogenation catalysts have been reported for almost all transition metals[1] and many heterogeneous catalysts are also known.[2] One of the roles of the catalyst is to activate the hydrogen molecule, i.e. to break or weaken the H–H bond via, for example, an oxidative addition of the hydrogen to the metal complex. In previous papers we have studied the oxidative addition of hydrogen to nickel[3] and the purpose of the present paper is to compare palladium and nickel with respect to the hydrogen addition reaction. The calculations on the $^1A_1$ state of NiH_2 showed that hydrogen is easily added to the naked nickel atom with a barrier of only 3 kcal/mol. NiH_2 forms a fairly stable complex with a binding energy of 8 kcal/mol and with a triangular bond between the three atoms. The nickel atom is dominated by a d^9 configuration along the whole potential surface.

From the differences in the nickel and palladium atomic spectra some differences in the binding to H_2 for the two metals can be predicted. The calculations on NiH_2 show that it is a singlet coupled d^9s configuration on nickel that forms the bonds to H_2.

(1) C. Masters, "Homogeneous Transition-Metal Catalysis", Chapman and Hall, London, 1981.
(2) G. C. Bond, "Heterogeneous Catalysis: Principles and Applications", Clarendon Press, Oxford, 1974.
(3) M. R. A. Blomberg and P. E. M. Siegbahn, *J. Chem. Phys.*, **78**, 986 (1983); *Ibid.*, in press.

0022-3654/84/2088-4617$01.50/0